Can Polymer Coils Be Modeled as "Soft Colloids"?

A. A. Louis,[1] P. G. Bolhuis,[1] J. P. Hansen,[1] and E. J. Meijer[2]
[1]*Department of Chemistry, Lensfield Road, Cambridge CB2 1EW, United Kingdom*
[2]*Department of Chemical Engineering, University of Amsterdam, Nieuwe Achtergracht 166, NL-1018 WV Amsterdam, The Netherlands*
(Received 26 May 2000)

We map dilute or semidilute solutions of nonintersecting polymer chains onto a fluid of "soft" particles interacting via a concentration dependent effective pair potential, by inverting the pair distribution function of the centers of mass of the initial polymer chains. A similar inversion is used to derive an effective wall-polymer potential; these potentials are combined to successfully reproduce the calculated exact depletion interaction induced by nonintersecting polymers between two walls. The mapping opens up the possibility of large-scale simulations of polymer solutions in complex geometries.

PACS numbers: 61.25.Hq, 61.20.Gy, 82.70.Dd

A statistical description of polymer solutions in complex geometries, such as the colloid-polymer mixtures which have recently received much experimental attention [1–3], generally relies on a nanometer scale segment representation of the polymer coils, a computationally very demanding task except in the special case of ideal (nonintersecting) polymers obeying Gaussian statistics [4]. This obviously follows from the fact that, although the colloidal particles may reasonably be modeled by hard impenetrable spheres or other complex shapes lacking internal structure, each polymer coil involves L segments which must satisfy a nonintersection constraint. It thus appears natural to attempt a mesoscale coarse graining, whereby polymer coils interact via effective pair potentials acting between their centers of mass (CM). Since polymers can interpenetrate, the effective potential $\beta v(r)$ is expected to be soft, with a range of the order of the radius of gyration R_g of individual coils. Such a coarse-grained description has been a long-time goal in the statistical mechanics of polymer solutions, dating back to the first attempts by Flory and Krigbaum [5] who employed mean-field theory to find an interaction for which the strength at overlap scales as $\beta v(r = 0) \sim L^{0.2}$. Later, scaling arguments [6], field-theoretical renormalization group calculations [7], and simulations [8] confirmed that the range of the interaction between two isolated polymer coils is of the order of R_g, but found that in the scaling limit the strength $\beta v(r = 0)$ is independent of L and of order k_BT.

In this Letter, we show that a meaningful "soft colloid" picture of polymer coils may be built on a coherent "first principles" statistical mechanical foundation. We derive both the effective wall-polymer CM interaction $\beta\phi(z)$, and the "best" local effective pair potential $\beta v(r)$ between polymer CM's for *finite* polymer concentrations. These potentials are then applied to simulate bulk polymer solutions, as well as inhomogeneous polymers near a hard wall and polymers confined between two parallel walls to extract the effective depletion potential between plates. The soft colloid approach turns out to be successful not only in the dilute regime but also, perhaps more surprisingly, well into the semidilute regime. A related "soft particle" picture has been applied to polymer melts and blends [9], but the corresponding phenomenological implementation differs substantially from the present first principles approach.

We consider a popular model for polymers in a good solvent [10], namely, N excluded volume polymer chains of L segments undergoing nonintersecting self-avoiding walks (SAW) on a simple cubic lattice of M sites, with periodic boundary conditions. The packing fraction is equal to the fraction of lattice sites occupied by polymer segments, $c = N \times L/M$, while the concentration of polymer chains is $\rho = c/L = N/M$. For a single SAW chain, the radius of gyration $R_g \sim L^{\nu}$, where $\nu \simeq 0.6$ is the Flory exponent [10]. The overlap concentration ρ^*, signaling the onset of the semidilute regime, is such that $4\pi\rho^* R_g^3/3 \simeq 1$, and hence $\rho^* \sim L^{-3\nu}$. We have carried out Monte Carlo (MC) simulations for chains of length $L = 100$ and $L = 500$, and covered a range of concentrations up to $\rho/\rho^* \sim 5$. The pair distribution function $g(r)$ of the centers of mass was computed for several concentrations; $g(r = 0)$ is always nonzero, thus confirming the "softness" of the effective pair potential $\beta v(r)$. The latter was then derived from $g(r)$ by an inversion procedure based on the hypernetted-chain (HNC) approximation closure relation [11]:

$$g(r) = \exp\{-\beta v(r) + g(r) - c(r) - 1\}, \qquad (1)$$

where $\beta = 1/k_BT$, while $c(r)$ is the direct pair correlation function, related to $g(r)$ by the Ornstein-Zernike (OZ) relation [11]. To any given $g(r)$ and density there corresponds a *unique* effective pair potential $\beta v(r)$, capable of reproducing the input $g(r)$, *irrespective of the underlying many-body interactions* in the system [12]; in a variational sense this $\beta v(r)$ provides the best pair representation of the true interactions [13], and leads back to the true thermodynamics via the compressibility relation [11]. While the simple HNC inversion procedure would be inadequate for dense fluids of hard-core particles, where more sophisticated closures or iterative procedures are required [13],

 0031-9007/00/85(12)/2522(4)$15.00

we are able to demonstrate the consistency of the HNC inversion in the present case [14]. If the resulting effective $\beta v(r)$, examples of which are shown in Fig. 1, are used directly in MC simulations, the calculated "exact" $g(r)$ for this effective representation coincides within statistical errors with the $g(r)$ derived from the simulation of the full initial polymer segment model. In fact, the HNC closure turns out to be quasiexact when applied to the simple Gaussian model [15] whereby particles interact via the potential $\beta v(r) = \epsilon \exp[-\alpha(r/R_g)^2]$, which yields a reasonable fit to the effective pair potentials shown in Fig. 1. Even the much cruder random-phase approximation closure, $c(r) = -\beta v(r)$, yields semiquantitatively accurate results in the regime of interest [16,17]. Careful inspection of Fig. 1 reveals that the effective pair potential is not very sensitive to the polymer concentration. The value at $r = 0$ first increases slightly with ρ, before decreasing again at the highest concentration. More strikingly, and perhaps not surprisingly, the range of $\beta v(r)$ increases with ρ. The effective potential becomes slightly negative $[\mathcal{O}(10^{-3}k_BT)]$ for $r/R_g \gtrsim 3$ at the higher concentrations.

The properties of soft-core fluids are significantly different from their hard-core counterparts. For example, for potentials of the type shown in Fig. 1, the pressure is very well described by $\beta P = \rho + 1/2\beta\hat{V}(0)\rho^2$ over the entire density range [16,17]. Here $\hat{V}(0)$ is the Fourier transform of the potential, at $k = 0$. Our observation that potentials become slightly longer ranged at higher densities implies that the pressure scales with an exponent slightly higher than 2, so that the equation of state (e.o.s.) is consistent with the well-known $\rho^{2.25}$ law [10], and reproduces the e.o.s. of the full SAW simulations [16]. At first sight it may seem surprising that a two-body potential could reproduce the full e.o.s. without explicit many-body terms. However, the effective potential we use is *constructed to reproduce the true thermodynamics* through the compressibility relation (ignoring small volume terms); the relative insensitivity of $\beta v(r)$ to concentration implies that many-body interactions are not very important [16].

This insensitivity to concentration makes it possible to apply the effective potential appropriate for a given mean concentration to inhomogeneous cases, where the local polymer concentration deviates from the mean. Such a situation occurs when a polymer solution is confined by a hard wall. Using the same explicit SAW polymer model in MC simulations, we have computed the exact profiles $h(z) = \rho(z)/\rho - 1$, where z denotes the perpendicular distance of the polymer CM from the wall. Examples of $h(z)$ for several bulk concentrations are shown in the inset of Fig. 2. The corresponding adsorptions Γ are defined by

$$\Gamma = -\frac{\partial(\Omega^{\mathrm{ex}}/A)}{\partial\mu} = \rho\int_0^\infty h(z)\,dz\,, \qquad (2)$$

where Ω^{ex}/A is the excess grand potential per unit area, ρ the bulk concentration of the polymers, and μ their chemical potential. From a knowledge of the concentration profile $\rho(z)$, and the bulk direct correlation function between polymers CM's $c(r)$, one may extract an effective wall-polymer potential $\beta\phi(z)$ by combining the wall-polymer OZ relations [11] with the HNC closure, resulting in

$$\beta\phi(z) = \beta\phi^{\mathrm{MF}}(z) + \rho\int d\mathbf{r}'\,h(z')c(|\mathbf{r} - \mathbf{r}'|)\,. \qquad (3)$$

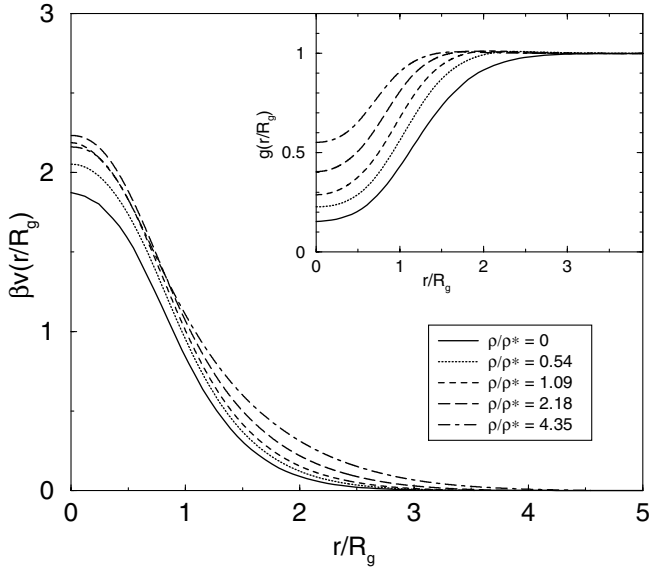

FIG. 1. The effective polymer CM pair potential $\beta v(r/R_g)$ derived from an HNC inversion of $g(r/R_g)$ for different densities. The x axis denotes r/R_g, where R_g is the radius of gyration of an isolated SAW polymer. Inset: The polymer CM pair distribution function $g(r)$ calculated for $L = 500$ SAW polymers and used to generate $\beta v(r)$.

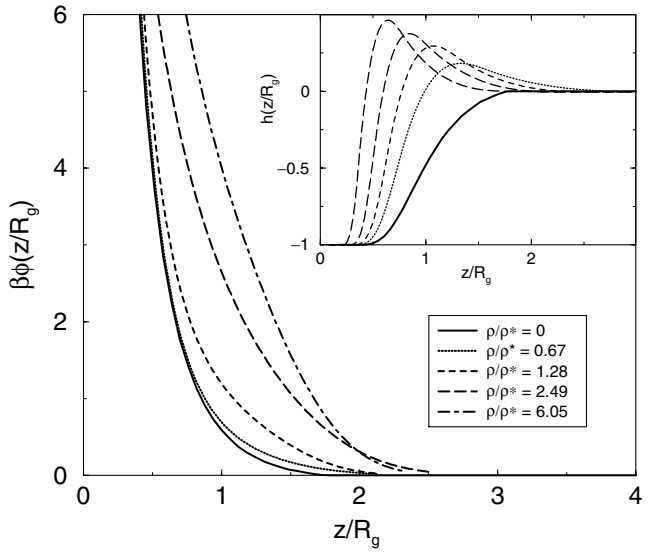

FIG. 2. The wall-polymer potential $\beta\phi(z/R_g)$ derived from an HNC inversion of $h(z)$. Inset: The wall-polymer density profile $h(z) = \rho(z)/\rho - 1$ for different densities. The corresponding adsorptions Γ are 0, 0.096, 0.132, 0.178, and 0.248 in units of R_g^{-2}, respectively.

The first term is the usual potential of mean force $\beta\phi^{\mathrm{MF}}(z) = -\ln[\rho(z)/\rho]$, to which $\beta\phi(z)$ would reduce in the $\rho \to 0$ limit, while the second term arises from correlations between the polymer coils next to the wall. Using the $c(r)$ extracted from the earlier bulk simulations of $g(r)$, together with Eq. (3), we are able to extract $\beta\phi(z)$ from the density profiles. Results for various bulk concentrations are plotted in Fig. 2. The range of the effective wall-polymer repulsion increases with increasing concentration, while the density profiles actually move in closer to the wall. It is important to stress that the correlation term considerably enhances the repulsion compared to the potential of mean force. We have tested the consistency of the inversion procedure (which, to the best of our knowledge, has not been attempted before for any wall/fluid interface) by using $\beta\phi(z)$, and the pair potential $\beta v(r)$ for the appropriate bulk concentration, in MC simulations based on these effective interactions (such simulations are at least an order of magnitude faster than simulations of the initial segment model). The resulting concentration profile of the effective soft colloids agrees to within statistical accuracy with the initial $\rho(z)$ obtained from the detailed segment simulations, and the corresponding adsorption Γ differs by less than 1% from the exact value, thus demonstrating the adequacy of the soft colloid representation of the interacting polymer coils.

An even more severe test of this representation is provided by a calculation of the depletion interaction between two hard walls confining the polymers within a slit of width d. Using direct grand-canonical simulations of the full SAW polymer model, we computed the osmotic pressure exerted by the polymer coils on the walls; the interaction free energy per unit area A, $\beta\Delta F/A$, is then obtained by integrating the osmotic pressure calculated for different values of the spacing d between the walls. These simulations are extremely computer intensive, and were carried out only for $L = 100$ [18]. In the soft colloid picture, the interactions of the polymer CM's with each other, $\beta v(r)$, and with a wall, $\beta\phi(z)$, are calculated once with the HNC inversion procedures from the $g(r)$ and $\rho(z)$ of a full SAW polymer simulation at the bulk density. These are then used in grand-canonical MC simulations of soft particles between two walls, and in Fig. 3 they are compared to the exact grand-canonical MC simulations of $L = 100$ SAW polymers (for $\rho/\rho^* = 0.95$). The results are in good agreement, but the soft colloid calculations are at least 2 orders of magnitude faster. Contrary to the more widely studied case of colloid-colloid mixtures [19], the exact interaction exhibits no significant repulsive barrier, while the soft colloid model leads to a flat maximum; the corresponding barrier height is, however, very small compared to the attractive minimum at contact, which agrees well with the exact data, as does the slope of the attraction. In fact, the repulsive barrier does not increase significantly with density [16], and its origin can be traced to our use of the "potential overlap approximation," namely,

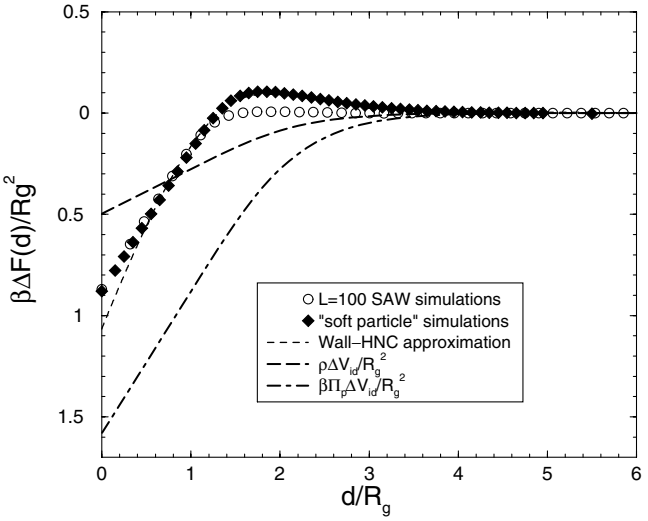

FIG. 3. Depletion free energy $\beta\Delta F(d)/R_g^2$ for two plates separated by d. Circles are the "exact" MC simulations of SAW polymers, the diamonds denote MC simulations of the "soft particles," the short dashed line denotes the wall-HNC approximation of Eq. (4). The long-dashed and dash-dotted lines denote the AO approximations mentioned in the text.

that the interaction of the soft particles with two parallel walls a distance d apart can be written as the sum of the two individual wall-particle interactions. This is exact for simple liquids with true intermolecular interactions, but not for polymers described by effective potentials, even if the polymers are ideal [16]. For the sake of consistency, the MC simulations for the soft colloid model were carried out with effective wall-polymer and polymer-polymer potentials appropriate for $L = 100$. However, we checked that the data obtained with effective interactions appropriate for longer polymers ($L = 500$), which cannot be easily handled within the full segment model, are very close to the $L = 100$ results, so we are confident that we are close to the scaling regime for properties of interest.

In Fig. 3 we also compare two results derived in the spirit of the Asakura-Oosawa (AO) approximation [20]. The free-energy difference $\beta\Delta F(z)$ is modeled by the density times the exact depletion volume, $\Delta V_{\mathrm{id}}(z)$, excluding one ideal Gaussian polymer of size R_g, or by a popular phenomenological improvement [1]: $\beta\Delta F(z) = \beta\Pi_b\Delta V_{\mathrm{id}}(z)$, where Π_b is the bulk osmotic pressure of the interacting polymers. Note that for the density under consideration, these approximations are seen to be very poor, both in regards to the depth and the range of the depletion attraction. In fact, the range of the depletion interaction for interacting polymer coils is significantly reduced compared to the AO predictions, valid for ideal polymers. For low densities we find, as expected, that all the above approaches converge [16].

These observations can be understood within the soft colloid representation and the HNC approximation [21], where the interacting free energy per unit area is

given by

$$\frac{\beta\Delta F(z)}{A} = -\rho\int_{-\infty}^{\infty} h(s)h(z-s)\,ds + \rho\int_{-\infty}^{\infty} h(z-s)[\beta\phi(s) - \beta\phi^{\mathrm{MF}}(s)]\,ds\,. \quad (4)$$

Here $h(z) = \rho(z)/\rho - 1$ is the *single wall* density profile, $\beta\phi(z)$ is the corresponding effective wall-polymer potential, and $\beta\phi^{\mathrm{MF}}(z)$ is the corresponding potential of mean force. The first term on the right-hand side of Eq. (4) is the density overlap approximation and would be the only contribution in the case of ideal (Gaussian) polymer coils. The second term arises from the correlations between coils; this dominates the first term in the semidilute regime ($\rho/\rho^* \geq 1$). The standard AO approximation [20] may be derived from Eq. (4) by replacing the density profile by a step function of width R_g in the first term of Eq. (4) and neglecting the correlation term. In Fig. 3 we compare the HNC approach of Eq. (4) for the wall-wall interaction to the exact results and the MC simulations of the soft colloids. As was found for the homogeneous case and for the single wall, HNC works very well here, demonstrating that knowledge of $\beta v(r)$ and $\beta\phi(z)$ quickly leads to accurate predictions for the slit geometry, paving the way for the use of integral equation techniques in other, more complex, geometries.

To summarize, the coarse-grained representation of polymer coils as soft colloids has been shown to be very reliable, yielding pair distribution functions and concentration profiles which agree closely with the results for the full SAW segment model, while being much more efficient from a computational point of view. Much of the success of the coarse graining lies in our finding that the best effective pair potential between CM's of neighboring coils does not depend strongly on polymer concentration, and is reasonably close to its $\rho \to 0$ limit. Similar conclusions were reached in recent work on the phase behavior of star polymers, where the $\rho \to 0$ limit of the pair potential was used to calculate the phase behavior at finite concentration [22]. Our results for the linear polymer case suggest that the full pair potential for star polymers may not be strongly concentration dependent, and that our approach could be used for star polymers in confined geometries.

Finally, we note that the soft colloid description is expected to work best in complex geometries where the curvature is not too large on the scale of R_g, such as colloid-polymer mixtures where the colloid radius $R \leq R_g$. For such systems, the soft colloid model may now be used in large-scale simulations or fluid integral equations of polymers in complex geometries, such as the structure [23], phase behavior [1], interactions [2], and metastability [3] of colloid-polymer mixtures, which cannot be achieved with the detailed model of nonintersecting polymer chains.

A. A. L. acknowledges support from the Isaac Newton Trust, Cambridge, P. G. B. acknowledges support from the EPSRC under Grant No. GR/M88839, and E. J. M. acknowledges support from the Royal Netherlands Academy of Arts and Sciences. We thank David Chandler, Daan Frenkel, Christos Likos, Hartmut Löwen, and Patrick Warren for helpful discussions.

[1] S. M. Ilett, A. Orrock, W. C. K. Poon, and P. N. Pusey, Phys. Rev. E **51**, 1344 (1995).
[2] R. Verma, J. C. Crocker, T. C. Lubensky, and A. G. Yodh, Phys. Rev. Lett. **81**, 4004 (1998).
[3] W. C. K. Poon *et al.,* Phys. Rev. Lett. **83**, 1239 (1999).
[4] E. J. Meijer and D. Frenkel, Phys. Rev. Lett. **67**, 1110 (1991); J. Chem. Phys. **100**, 6873 (1994).
[5] P. J. Flory and W. R. Krigbaum, J. Chem. Phys. **18**, 1086 (1950).
[6] A. Y. Grosberg, P. G. Khalatur, and A. R. Khokhlov, Makromol. Chem. **3**, 709 (1982).
[7] B. Krüger, L. Schäfer, and A. Baumgärtner, J. Phys. (Paris) **50**, 319 (1989).
[8] J. Dautenhahn and Carol K. Hall, Macromolecules **27**, 5399 (1994), and references therein.
[9] M. Murat and K. Kremer, J. Chem. Phys. **108**, 4340 (1998).
[10] M. Doi, *Introduction to Polymer Physics* (Oxford University Press, Oxford, 1995).
[11] J. P. Hansen and I. R. McDonald, *Theory of Simple Liquids* (Academic Press, London, 1986), 2nd ed.
[12] R. L. Henderson, Phys. Lett. **49A**, 197 (1974); J. T. Chayes and L. Chayes, J. Stat. Phys. **36**, 471 (1984).
[13] L. Reatto, Philos. Mag. A **58**, 37 (1986); L. Reatto, D. Levesque, and J. J. Weis, Phys. Rev. A **33**, 3451 (1986).
[14] To do the inversion we perform SAW simulations on a ($M = 120 \times 120 \times 120$) cubic lattice with periodic boundaries. The number N of polymers ($L = 500$ segments each) ranges from 50 to 500. For the polymer-wall interaction we employed a $M = 160 \times 100 \times 100$ lattice with the wall perpendicular to the long axis.
[15] F. H. Stillinger, J. Chem. Phys. **65**, 3968 (1976).
[16] A. A. Louis, P. Bolhuis, and J. P. Hansen, cond-mat/0007062; P. G. Bolhuis, A. A. Louis, J. P. Hansen, and E. J. Meijer (to be published).
[17] A. Lang, C. N. Likos, M. Watzlawek, and H. Löwen, J. Phys. Condens. Matter **12**, 5087 (2000).
[18] For details of the simulations see E. J. Meijer *et al.* (to be published).
[19] Y. Mao, M. E. Cates, and H. N. W. Lekkerkerker, Physica (Amsterdam) **222A**, 10 (1995); B. Götzelmann, R. Roth, S. Dietrich, M. Dijkstra, and R. Evans, Europhys. Lett. **47**, 398 (1999); S. Melchionna and J. P. Hansen, Phys. Chem. Chem. Phys. **2**, 3465 (2000).
[20] S. Asakura and F. Oosawa, J. Chem. Phys. **22**, 1255 (1954); A. Vrij, Pure Appl. Chem. **48**, 471 (1976).
[21] P. Attard, D. R. Bérard, C. P. Ursenbach, and G. N. Patey, Phys. Rev. A **44**, 8224 (1991).
[22] M. Watzlawek, C. N. Likos, and H. Löwen, Phys. Rev. Lett. **82**, 5289 (1999).
[23] A. A. Louis, R. Finken, and J. P. Hansen, Europhys. Lett. **46**, 741 (1999).